Classification: Biological sciences- plant biology.

Impaired respiration discloses the physiological significance of state transitions in Chlamydomonas.

Pierre Cardol[1], Jean Alric[2], Jacqueline Girard-Bascou[2], Fabrice Franck[3], Francis-André Wollman[2,*], Giovanni Finazzi[2,*]

[1]Laboratoire de Génétique des Microorganismes et [3]Laboratoire de Photobiologie, Département des Sciences de la Vie, 27, Bld du rectorat, Université de Liège, B-4000 Liège, Belgique [2] Institut de Biologie Physico-Chimique, Unité Mixte de Recherche 7141, CNRS and UPMC- Université Paris 6, 13 rue Pierre et Marie Curie, 75005, Paris, France

***corresponding authors:**

Francis André Wollman

Institut de Biologie Physico-Chimique

13, rue Pierre et Marie Curie, 75005 Paris, France

Phone: +33 [0]1 58 41 50 12

Fax: +33[0]1 58 41 50 22

Francis-Andre.Wollman@ibpc.fr

Giovanni Finazzi

Institut de Biologie Physico-Chimique

13, rue Pierre et Marie Curie, 75005 Paris, France

Phone: +33 [0]1 58 41 51 01

Fax: +33[0]1 58 41 50 22

giovanni.finazzi@ibpc.fr

ms information: 17 pages, 3 figures, 1 table, 3 supporting figures, 1 supporting table, 1 supporting methods.

Abbreviations: CEF cyclic electron flow; Chl, chlorophyll; DCMU, 3-(3',4'-dichlorophenyl)-1,1-dimethylurea; ECS, electrochromic shift; PQ: plastoquinone; PS, photosystem; P_{700}: primary electron donor of Photosystem I; ST: state transitions.

ABSTRACT

State transitions correspond to a major regulation process for photosynthesis, whereby chlorophyll protein complexes responsible for light harvesting migrate between photosystem II and photosystem I in response to changes in the redox poise of the intersystem electron carriers. Here we disclose their physiological significance in *Chlamydomonas reinhardtii* using a genetic approach. Using single and double mutants defective for state transitions or/and mitochondrial respiration, we show that photosynthetic growth, and therefore biomass production, critically depends on state transitions in respiratory defective conditions. When extra ATP cannot be provided by respiration, enhanced PSI turnover elicited by transition to state 2 is required for photosynthetic activity. Concomitant impairment of state transitions and respiration decreases the overall yield of photosynthesis, ultimately leading to reduced fitness. We thus provide experimental evidence that the combined energetic contributions of state transitions and respiration are required for efficient carbon assimilation in this alga.

\body **INTRODUCTION**

State transitions (ST) are a short term photosynthetic acclimation process that controls the reversible association of the PSII antenna protein complex (LHCII) with either photosystem (PS)II (in state 1) or PSI (in state 2) (reviews in (1-3)). This relies on the reversible LHCII phosphorylation involving the Stt7-STN7-membrane-bound protein kinase, which has been recently identified in *Chlamydomonas reinhardtii* and *Arabidopsis thaliana* (4, 5). Phosphorylation changes lead to the migration of a fraction of the antenna between the PSII-enriched membrane domains and the PSI-enriched membrane domains within the thylakoids in plant and algal chloroplasts (reviewed in (3, 6)).

ST were first observed in unicellular green algae, and originally described as a mechanism linking the redox poise of the intersystem electron carriers to changes in absorption capacity of the photosystems (3). Reduction of the plastoquinone (PQ) pool upon increased PSII sensitization activates the kinase *via* the cytochrome b_6f complex (7). Conversely, PQH_2 oxidation, upon increased PSI sensitization, inactivates the kinase. P_i-LHCII is then dephosphorylated by a phosphatase (3), whose biochemical nature and regulation remain elusive.

In plants, ST are of limited amplitude, involving ~ 20% of LHCII (8). Their occurrence is likely unessential for plant survival, as suggested by the very limited effects on growth (4, 9-11), and on fitness (12) of a mutation preventing ST in Arabidopsis. This mutant only shows a marked phenotype under a very particular fluctuating light regime (*e.g.* (4)). In Chlamydomonas, ST involve a larger fraction of PSII antenna than in plants, with ~ 80% of PSII antennae being implicated in this phenomenon (13), including monomeric LHCII (14). The very large redistribution of light harvesting complexes upon ST in this alga is difficult to reconcile with a mere role of balancing light absorption. Indeed, the huge decrease in PSII absorption (by a factor of ~ 2) leads to unbalanced PSI and PSII absorption capacity in state 2, (see *e.g.* (15), for a discussion). This large energy redistribution between the two photosystems largely favors PSI photochemistry at the expense of PSII in light limiting conditions. Based on a number of experiments, it was then concluded that ST in Chlamydomonas rather served to change the ratio between linear and cyclic electron flow around PSI (reviewed in (2)). It came thus as a surprise that there was no specific growth defect in mutants lacking the STT7 kinase that controls ST in Chlamydomonas (16).

A tight interplay between respiratory activity and ST has been reported earlier in dark-adapted Chlamydomonas. This interplay was documented using inhibitors of mitochondrial respiration or upon analysis of respiratory-deficient mutants (17, 18). In both cases, impaired respiration depleted intracellular ATP pools in the dark, which stimulated glycolysis according to the "Pasteur effect". Released reductants in the chloroplast stroma enhanced non photochemical reduction of the PQ pool in the thylakoid membranes, favoring acclimation to state 2 in darkness. Subsequent illumination restored ATP cellular levels, allowed partial reoxidation of plastoquinone pool and transition to state 1. Based on these earlier observations, we decided to explore the possible role of ST on photosynthesis in Chlamydomonas in relationship to changes in respiratory efficiency. Therefore, we took a genetic approach to compare photosynthetic efficiencies in mutants impaired in respiration or/and in state transitions.

RESULTS

The absence of state transitions in a respiration defective context is detrimental for cell growth in Chlamydomonas. We first assessed the possible interplay between ST and respiration during illumination, by comparing growth of the ST-competent wild type and the ST-defective *stt7-9* mutant under photoautotrophic and mixotrophic conditions. As indicated by the growth on solid media (Fig. 1A) or by the doubling times in liquid cultures (Fig. 1B) there were no significant differences between the two strains (see also (16)). This suggests that state transitions are dispensable for biomass generation in these experimental conditions, where both photosynthesis and respiration are fully active. Addition of myxothiazol, a known inhibitor of mitochondrial respiration, led to growth decrease in mixotrophic conditions in the two strains, consistent with the prominent role of respiration in acetate assimilation. Nevertheless, a larger effect was seen in *stt7-9*, suggesting a possible specific inhibitory effect in this strain. Consistent with this hypothesis, a marked contrast became apparent between the growth rates of the two strains when the respiratory inhibitor myxothiazol was added in photoautotrophic conditions. Myxothiazol drastically reduced growth in *stt7-9* cells (Fig. 1A and B), whereas it had only a marginal effect in wild-type cells, suggesting that efficient photosynthetic growth requires respiration in the absence of ST.

This observation prompted us to use a genetic approach to further explore the interplay between ST and respiration. We resorted to Chlamydomonas mutants defective in mitochondrial activity (*dum*'s, reviewed in (19)) to generate a double mutant impaired in both ST and mitochondrial respiration. To this end, we crossed the *dum22* mt^- mitochondrial mutant -lacking both complex I and III activities- with the *stt7-9* mt^+ nuclear mutant devoid of ST because of the absence of the Stt7 kinase. We isolate 7 *dum22 stt7-9* clones defective in state transitions and in mitochondrial respiration (see Fig. S1A, S1B, Table S1 and supplementary Methods). We then compare them with their parental strains for growth capacity in photoautotrophic and mixotrophic conditions (Fig. 1C, Fig. S1C). In line with the observations drawn from the use of respiration inhibitors, we found that the combined defects in respiration and state transitions led to a severe decrease in growth rates. We first ruled out the possibility that the growth defect could originate from an increased photosensitivity. Indeed *dum22 stt7-9* did not show further growth inhibition in phototrophic conditions upon increasing the light intensity (Fig. 1C). In addition, no statistically significant differences in photosensitivity were seen when measuring changes in the photosynthetic efficiency (Fv/Fm) in wild type, *stt7-9*, *dum22* and *dum22 stt7-9* cells exposed to saturating light (Fig. S2). Thus, we conclude that some metabolic features of *dum22 stt7-9* are limiting for growth rate in photoautotrophic conditions.

Functional characteristics of dum22 stt7-9. In order to understand which factors limit the *dum22 stt7-9* growth rate in photoautotrophic conditions, we further characterized its photosynthetic properties. Recent data have suggested that ST may contribute to long term acclimation, via the regulation of gene expression (9, 10). In particular, it has been suggested that ST may modulate the relative amounts of active PSI and PSII in plants acclimated to either state 1 or state 2 (*e.g.* (20)). To test possible changes in the RC stoichiometry in *dum22* cells, which are acclimated to state 2 (18), and *stt7-9* and *dum22 stt7-9* cells, which are, in principle, locked in state 1 (5), we used a spectroscopic approach based on the amplitude of the light-induced electrochromic shift (ECS). This technique has already been employed successfully to evaluate the PSI/PSII stoichiometry in freshwater green algae (*e.g.* (21)). As shown in Fig. 2A, very minor differences were seen between the different strains, suggesting that the absence of ST has no significant effect on the RC stoichiometry, at least in Chlamydomonas (see also (1)).

We next assessed the balance in light energy distribution between the two photosystems that should be affected due to the inability of *stt7-9* and of *dum22 stt7-9* to perform ST. We first

evaluated the PSII antenna in cells dark-adapted for ~30 minutes after being grown photoautotrophically in low light (*i.e.* conditions where the growth phenotype of *dum22 stt7-9* cells is maximum). To this aim, we measured the rate of chlorophyll fluorescence induction from open (F_0) to closed PSII centers (F_m) in the presence of DCMU. This parameter, which is quantitatively related to the absorption cross section of this photosystem (*e.g.* (22)) was two times slower in *dum22* (Fig 2B) than in *dum22 stt7-9*, *stt7-9* and wild type cells. In addition, illumination of *dum22* in the presence of DCMU for 10 minutes (a treatment known to promote transition to state 1 via oxidation of the plastoquinone pool (17, 18)) increased its rate of fluorescence induction to values close to those measured in the other strains, whereas such a treatment has no effect on *dum22 stt7-9* cells (Fig. 2C). Consistent with this, the ratio of PSI/PSII fluorescence emission at 77K was higher in *dum22* than in the other strains in aerobic conditions, but it decreased to similar values when illuminated in the presence of DCMU (Sup. Table 1). Altogether, these data confirm that *dum22 stt9-7* mutant was mostly in state 1 conditions, because it lacks the Stt7 kinase, while *dum22* mutant was in state 2. We next assessed changes in PSI antenna, by measuring the light saturation curve for P_{700} oxidation (23). Dark-adapted cells, placed in aerobic conditions, were exposed to a laser flash (duration 5 ns) of variable intensity, and the light-induced oxidation of P_{700}, the primary electron donor of PSI, was estimated from the amplitude of the 4µs component of the decay-associated spectra of P_{700}^+ (*e.g.* (24)). As shown in Fig. 2D, a larger P_{700} oxidation was observed in *dum22* cells upon excitation with limiting light intensities. This indicates that the twofold decreased in PSII absorption capacity - due to state 2 acclimation - was accompanied by an increase in the PSI antenna size of similar extent, in agreement with previous functional (13) and biochemical (14) studies in wild type cells.

Increasing the PSI absorption capacity at the expense of PSII, as observed in *dum22,* should lead to unbalanced excitation of the two photosystems at limiting photon flux. To evaluate this possibility, we measured the redox state of P_{700} in steady state continuous illumination. Again, experiments were conducted in conditions where growth was mostly affected in *dum22 stt7-9* mutant, *i.e.* upon photoautotrophic growth in low light. Furthermore, we added an artificial PSI electron acceptor methylviologen (MV, 2mM), to avoid any kinetic limitation by the PSI acceptor side, and/or to avoid accumulation of reduced ferredoxin, and NADPH, which may lead to electron re-injection into the intersystem electron carriers through cyclic flow (*e.g.* (25)). Fig. 3A shows typical kinetics of P_{700} oxidation in wild type, *stt7-9*, *dum22* and *dum22 stt7-9* using

continuous illumination of limiting (50 µmol photons m^{-2} s^{-1}, open symbols) and saturating (800 µmol photons m^{-2} s^{-1}, closed symbols) intensity. These traces were employed to estimate the light saturation profiles of P_{700} oxidation in the four strains. As shown by the large difference in these profiles (Fig. 3B), photon absorption was unbalanced in favor of PSI in *dum22*, consistent with the transfer of light harvesting antenna from PSII to PSI, when compared to the other three strains. Addition of the PSII inhibitor DCMU to MV-treated cells largely enhanced P_{700} oxidation (Fig S3), confirming that most of the electrons delivered to P_{700}^{+} were of PSII origin. We note however an incomplete oxidation of P_{700} at low light intensities in all strains in the presence of both chemicals. We tentatively attribute this DCMU insensitive electron pathway to the NDH-mediated chlororespiratory pathway (26, 17)). Using the same procedure employed to evaluate the rate of electron flow in DCMU poised cells (see table I below), we evaluate the maximum electron flow capacity of this pathway to ~ 2-3 electrons/PSI/sec in wild type cells.

Light-dependent plus enhanced light-independent plastoquinone reduction decreases photosynthetic yield at low light in dum22 stt7-9. We next tested the overall photosynthetic activity by measuring oxygen evolution and fluorescence changes at different light intensities in wild type, *stt7-9*, *dum22* and *dum22 stt7-9* cells in photoautotrophic conditions. In all strains, very similar maximum oxygen evolution rates were observed (Fig 3C). However, a drastic inhibition of photosynthesis (65% to 75%) appeared in *dum22 stt7-9* cells at limiting light intensities, whereas it decreased by only ~ 35 % in *dum22* when compared to wild type and *stt7-9* cells (inset). The reduced photosynthetic activity in *dum22 stt7-9* was also accompanied by a drop in the quantum yield of linear electron flow as measured by the fluorescence parameter ΦPSII (27) (Fig. 3D). This experiment reveals that efficient photosynthesis cannot take place in a ST impaired mutant when respiration is inhibited in Chlamydomonas. However, the mere inhibition of ST is insufficient to modify photosynthesis when the stromal redox pressure is low, owing to sustained respiratory activity, as shown by the lack of phenotype in *stt7-9* cells. Thus, the rationale for the inhibition observed in *dum22 stt7-9* should be found in two processes that develop upon changes in the redox poise of the stromal compartment when respiration is inhibited. First, both the *dum22* and *dum22 stt7-9* mutants display a high level of non photochemical reduction of the plastoquinone pool due to the "Pasteur Effect" associated with their respiratory defect (see introduction). This large electron reservoir for PSI turnover is paralleled by a higher PSI light harvesting capacity in *dum22* only, because it undergoes a

transition to state 2, in contrast to *dum22 stt7-9*, which is locked in state 1 and keeps a small PSI antenna. It appears therefore that the rate of PSI driven oxidation of the plastoquinol pool in the *dum22 stt7-9* mutant cannot cope with its rate of PSII-driven photochemical reduction combined with enhanced rates of stromal-driven non photochemical reduction. This results in an accumulation of reducing equivalents among the intersystem electron carriers (Fig. 3B and D) and a drop in overall photosynthetic activity (Fig. 3C) and biomass production. Still, the enhanced reduction pressure from the stroma would be expected to enhance cyclic flow around PSI (CEF) (25). But the impairment of transition to state 2 in *dum22 stt7-9* should lead to a diminished CEF in light-limiting conditions because it keeps its PSI antenna smaller than in *dum22*. To test this hypothesis, we assess the efficiency of CEF by measuring the redox changes of P_{700} (using the same approach as in Fig. 3A) in the presence of the sole PSII inhibitor DCMU. PSII activity being prevented, the rate of P_{700} re reduction after illumination allows the determination of CEF (see *e.g.* (28)). The flow rate of this process (*i.e.* the number of electrons transferred per PSI per unit of time) was evaluated as $k * [P_{700}^+]/([P_{700}^+]+[P_{700}])$, where k is P_{700}^+ reduction rate after full oxidation by 10s of saturating light, and $[P_{700}^+]/([P_{700}^+]+[P_{700}])$ is the oxidation level at any light intensity. Table I shows that although the relative efficiency of CEF decreased at low light (50 μmol m^{-2} s^{-1}) in all strains, the CEF rate was much higher in *dum22* cells that were locked in state 2, when compared to the other strains that remained in state 1.

As CEF should contribute significantly to ATP synthesis upon illumination, we compared the steady state cellular ATP levels. Table 1 shows that despite changes in CEF and the overall photosynthetic activity, no differences in ATP levels were seen between *dum22* and *dum22 stt7-9* mutant cells in the light, in both mixotrophic and photoautotrophic conditions. As expected because of their respiratory deficiencies, the two strains showed ATP depletion upon dark incubation and a slightly lower ATP content in the light when compared to their wild type and *stt7-9* counterparts.

DISCUSSION

In plants, ST are regarded as a regulatory process of photosynthesis that optimizes linear electron flow by a proper balance of energy distribution between the two photosystems (3). In microalgae like Chlamydomonas, ST have been proposed to tune the ratio of cyclic to linear

electron flow in photosynthesis in response to changes in the intracellular demand for ATP (2). It was then somewhat paradoxical that the absence of ST in a phototrophic mutant of Chlamydomonas lacking the Stt7 kinase had no effect on its growth characteristics when compared to the wild type ((16) and the present study). This lack of growth phenotype can be better understood if the energetic contribution of the mitochondria, *i.e.* the other major cellular energy producer (besides the chloroplast) is taken into account. In algae, the tight metabolic interaction between the two bioenergetic compartments is exemplified by the modulation of the redox poise of the plastoquinone pool in the thylakoid membranes by the efficiency of respiration (18). In another instance, a second site suppressor mutant of a chloroplast ATP synthase mutant of Chlamydomonas (Fud50, (29)), which was still devoid of the chloroplast enzyme, could grow photoautotrophically, at variance with the original mutant strain. In this new genetic context, ATP exchange between the mitochondrion and the chloroplast became efficient enough to provide *all* the ATP required for photosynthetic CO_2 assimilation *in vivo.*

Here we showed that the ability to perform state transitions becomes critical for phototrophic growth in a respiration-deficient context. The double mutant *dum22 stt7-9*, lacking the Stt7 kinase and defective for respiration, is locked in state 1, *i.e.* in conditions where the absorption properties of both photosystems are similar (13). Although this should be ideally suited for electron flow from water to CO_2, *dum22 stt7-9* grows more slowly than *dum22*, *stt7-9* and wild-type strains in photoautotrophic conditions under limiting white light conditions. This phenotype can be rationalized as follows. *On the one hand*, non photochemical reduction of the plastoquinone pool by the thylakoid-located NDH (26) is rather efficient in mitochondrial mutants of Chlamydomonas. Therefore, concomitant electron injection into the pool by photochemical (PSII) and non photochemical (NDH) processes mimic an increase of PSII activity, which can only be counterbalanced at low light if PSI activity is enhanced. The massive increase in PSI absorption capacity (~ a factor of 2) in *dum22* cells due to constitutive acclimation to state 2 ((18) Fig. 2) highly favors PSI activity in low light. This allows re oxidation of the PQ pool, and efficient light utilization for biomass production. In contrast, more balanced light partitioning between PSII and PSI and over-reduction of the PQ pool in *dum22 stt7-9*, which is constitutively locked in state 1, becomes detrimental for light utilization at low photon density. This is shown by its reduced photosynthetic performance both in terms of oxygen evolution and of PSII efficiency, as derived from fluorescence emission (Fig. 3). Furthermore, the

increased PSI sensitization in state 2 conditions, observed in the *dum22* mutant but not in the *dum22 stt7-9* mutant, should be accompanied by an enhancement of cyclic flow at low light around this complex (18). Indeed, the CEF rate was much reduced in *dum22 stt7-9* when compared to that in *dum22* (table I). *On the other hand*, the Benson-Calvin cycle requires ATP and NADPH in a stoichiometry of 1.5, *i.e.* a ratio that cannot be entirely fulfilled by the sole operation of photosynthetic "linear electron flow". Recent estimates suggest that this process has an insufficient proton to electron balance, when compared to the stoichiometry of H^+ required to fuel ATP synthesis by the chloroplast CF_o-F_i complex (*e.g.* (30) see however (31)). In Chlamydomonas, it can be estimated that no more than 1.4 ATP should be synthesized per NADPH (≈ 1.39, *e.g.* (15)). Thus, even when light utilization is fully optimized, alternative processes must contribute to the generation of an "extra" ΔpH, *i.e.* of additional ATP synthesis to re-equilibrate the ATP/NADPH stoichiometry for proper carbon assimilation. Synthesis of ATP can be fueled by cyclic photophosphorylation, which does not require PSII activity (32) but also through the reduction of molecular oxygen by the Mehler reaction or the activity of the plastid terminal oxidase, PTOX (review in (33)). Mitochondria can also provide extra ATP while consuming reducing equivalents exported from the chloroplast via the malate or the triose phosphate transporter (reviewed in (34)).

Our present study, which shows no differences in photosynthesis (Fig. 3) and growth (Fig. 1) between the wild type and the *stt7-9* mutant impaired in ST, suggests that the mere inhibition of ST is not sufficient to impair biomass production through photosynthesis. Conversely, our results argue for a bioenergetic recruitment of mitochondria in relieving photosynthesis in the absence of ST-driven cyclic electron flow, by providing extra ATP for photosynthesis. The bioenergetic contribution of mitochondria to photosynthesis-driven metabolism is exemplified by the lower intracellular ATP levels in photoautotrophic conditions under low light when respiration is blocked (*dum22*), even if PSI turnover and growth rate are not compromised. It is of note that the ATP level reached upon exposure of *dum22* cells to low light is very close to that measured in the wild type in the dark. This suggests that in low light, photosynthesis in *dum22* is still capable of sustaining cell growth, while being already ATP-limited. Thus, state transitions in the absence of respiration promote enough CEF-driven ATP synthesis for growth but place the cells in an ATP limiting situation. Conversely, our observation that the ATP levels in *dum22 stt7-9* cells cannot be further decreased when compared to *dum22* (Table 1) strongly suggests that

below a threshold level, ATP becomes limiting for photosynthetic growth, in agreement with previous data (*e.g.* (35)). Thus, the limited energy supply at low light in the double mutant is likely consumed in intracellular metabolism at the expense of biomass production and cell division. Ultimately, this leads to a decrease in growth rate.

In conclusion, our study provides evidence for the contribution of the two major bioenergetic pathways to supply photosynthesis with "extra ATP" required for carbon assimilation in Chlamydomonas. Oxidative phosphorylation in mitochondria seems to play a prominent role not only in the dark to light transition as previously proposed for vascular plants (36) but also in steady state, light-limited conditions. Cyclic electron flow, which is boosted in state 2 conditions, also contributes to this process, and supplies ATP in the absence of energy supply by mitochondria. Owing to the existence of an intimate relationship between the cellular respiratory capacity, and the ability to modulate the PSI absorption cross section through state transitions, this results in a tight interplay between cyclic electron flow and respiration, which seems to be particularly effective in Chlamydomonas. It provides these unicellular organisms with a very high photosynthetic flexibility in terms of both ATP generation and electron transfer capacity in highly reducing conditions. This is certainly one of the major metabolic features enabling successful acclimation of this alga to its rapidly changing environmental conditions.

MATERIAL AND METHODS

Strains and growth conditions. The Chlamydomonas wild type strain used in this work is derived from the 137c strain (cc-1373 of the Duke University). Chlamydomonas *dum22* strain is a deletion mutant lacking the left telomere, the *cob* gene, and part of the *nd4* gene (reviewed in (19)). *Stt7-9* is a clone allelic to *stt7*, which can be easily crossed, at variance with the original strain (Gift from J.-D. Rochaix). Double mutants *dum22 stt7-9* were obtained by crossing the *dum22 mt*$^-$ mutant with a *stt7-9 mt*$^+$ mutant using standard procedures (see supplemental data for further information). Seven *dum22stt7-9* clones were isolated (Fig. S1). Two of them (A1, J1,) were further analyzed for their photosynthetic features. Cells were routinely cultivated at 50 µmol photons m^{-2} s^{-1} in mixotrophic (TAP) or photoautotrophic (Min) conditions.

Spectroscopy. Cells were harvested during exponential growth ($2*10^6$ cells per mL) and resuspended at a concentration of 10^7 cells mL^{-1} in minimum medium with addition of 20% (w/v) Ficoll to prevent cell sedimentation. *In vivo* kinetics measurements were performed at room

temperature with two different setups. Steady state P700 oxidation kinetics and RC stoichiometries were measured using a JTS spectrophotometer (Biologic, France). Continuous light was provided by a red source (630 nm), which was switched off transiently while measuring P_{700} absorption changes at 705 nm. PSI and PSII content was estimated spectroscopically from changes in the amplitude of the fast phase (100µs) of the ECS signal (at 520 nm – 545 nm) upon excitation with a saturating laser flash. The ECS spectral change follows linearly the number of light-induced charge separations within the reaction centres (37). Thus, PSII contribution can be calculated from the decrease in the signal amplitude upon addition of DCMU (20 µM) and hydroxylamine (1 mM) that irreversibly block PSII charge separation once the sample has been pre illuminated (21). Conversely, PSI was estimated as the fraction of the signal that was insensitive to these inhibitors. The light saturation profile of P700 oxidation (Fig 2 D) was measured with a second setup, having a time resolution of 10 ns. Actinic flashes were provided by a dye laser at 600 nm, the intensity of which were changes using neutral filters, whereas detecting flashes were provided by an optical parametric oscillator. The extent of P_{700} oxidation was evaluated from the 900 ns -20µs phase of absorption changes at 430-460 nm, in line with previously recorded spectra of the 4µs component of the decay-associated spectra of P_{700}^{+} in wild type cells (24). Fluorescence inductions were measured using a home built fluorometer. Excitation was provided by a green LED source (520 nm), and fluorescence was detected in the near IR region. PSII antenna size was evaluated by the rate of fluorescence induction in the presence of the PSII inhibitor DCMU. In the presence of this inhibitor, an average of 1 photon per PSII centre is absorbed at time *t* (*e.g.* (25). This parameter was estimated for every fluorescence induction trace to evaluate the number of absorbed photons. Fluorescence emission spectra at 77 K were recorded using a LS 50B spectrofluorometer (Perkin Elmer). Excitation was at 440 nm, and emission was detected at 685 nm (PSII) and 715 nm (PSI). Spectra were corrected for the wavelength-dependent photomultiplier response.

Oxygen evolution and ΦPSII. Oxygen evolution and the quantum yield of PSII in the light (ΦPSII (27)) were measured simultaneously using a Clark electrode connected to a modulated fluorometer (type MFMS, Hansatech Instruments, UK) in Min liquid medium supplemented with $NaHCO_3$ 5mM. ΦPSII was calculated as (Fm'-Fs)/Fm', where Fm' is the maximum fluorescence

emission level induced by a pulse of saturating light (~ 5000 µmol of photons m^{-2} s^{-1}) and Fs is the steady state level of fluorescence emission. Chl concentration was adjusted to 5 µg mL^{-1}.

ATP measurements. ATP was extracted as in (17) using 5% $HClO_4$. Samples were centrifuged at 15,000 rpm, and a volume of the supernatant was diluted in 0.5 M Tris-Acetate pH 7.75 (1/300, v/v). Determination of ATP content was made using the Enliten luciferase/luciferin kit (Promega, Madison, WI) with a Lumat LB9501 apparatus (Berthold).

ACKNOWLEDGEMENTS.

We thank Fabrice Rappaport for valuable suggestions. This work was supported by grants from the Belgian Fonds pour la Recherche Scientifique (F.R.S.-FNRS 1.C057.09 and F.4735.06 to PC) and from the "Centre National de la Recherche Scientifique" (CNRS). P.C. is F.R.S.-FNRS research associate.

REFERENCES

1. Rochaix JD (2007) Role of thylakoid protein kinases in photosynthetic acclimation. *FEBS Lett* **581:**2768-75.
2. Wollman FA (2001) State transitions reveal the dynamics and flexibility of the photosynthetic apparatus. *EMBO J* **20:**3623-30.
3. Allen JF (1992) How does protein phosphorylation regulate photosynthesis? *Trends Biochem Sci* **17:**12-7.
4. Bellafiore S, Barneche F, Peltier G, Rochaix JD (2005) State transitions and light adaptation require chloroplast thylakoid protein kinase STN7. *Nature* **433:**892-5.
5. Depege N, Bellafiore S, Rochaix JD (2003) Role of chloroplast protein kinase Stt7 in LHCII phosphorylation and state transition in Chlamydomonas. *Science* **299:**1572-5.
6. Gal A, Zer H, Ohad I (1997) Redox-controlled thylakoid protein phosphorylation : News and views. *Physiol Plant* **100:**869-85.
7. Wollman FA, Lemaire C (1988) Studies on kinase-controlled state transitions in photosystem II and b_6f mutants from *Chlamydomonas reinhardtii* which lack quinone-binding proteins. *Biochim Biophys Acta* **85:**85-94.
8. Allen J (2002) Photosynthesis of ATP-electrons, proton pumps, rotors, and poise. *Cell* **110:**273-6.
9. Tikkanen M, Piippo M, Suorsa M, Sirpio S, Mulo P, Vainonen J, Vener AV, Allahverdiyeva Y, Aro EM (2006) State transitions revisited-a buffering system for dynamic low light acclimation of Arabidopsis. *Plant Mol Biol* **62:**779-93.

10. Bonardi V, Pesaresi P, Becker T, Schleiff E, Wagner R, Pfannschmidt T, Jahns P, Leister D (2005) Photosystem II core phosphorylation and photosynthetic acclimation require two different protein kinases. *Nature* **437:**1179-82.
11. Lunde C, Jensen PE, Haldrup A, Knoetzel J, Scheller HV (2000) The PSI-H subunit of photosystem I is essential for state transitions in plant photosynthesis. *Nature* **408:**613-5.
12. Frenkel M, Bellafiore S, Rochaix JD, Jansson S (2007) Hierarchy amongst photosynthetic acclimation responses for plant fitness. *Physiol Plantarum* **129:**455-9.
13. Delosme R, Olive J, Wollman FA (1996) Changes in light energy distribution upon state transitions : as in vivo photoacoustic study of the wild-type and photosynthesis mutants from Chlamydomonas reinhardtii. *Biochim Biophys Acta* **1273:**150-8.
14. Takahashi H, Iwai M, Takahashi Y, Minagawa J (2006) Identification of the mobile light-harvesting complex II polypeptides for state transitions in Chlamydomonas reinhardtii. *Proc Natl Acad Sci U S A* **103:**477-82.
15. Eberhardt S, Finazzi G, Wollman FA (2008) The dynamics of photosynthesis. *Annu Rev Genet* **42:**463-515.
16. Fleischmann MM, Ravanel S, Delosme R, Olive J, Zito F, Wollman FA, Rochaix JD (1999) Isolation and characterization of photoautotrophic mutants of Chlamydomonas reinhardtii deficient in state transition. *J Biol Chem* **274:**30987-94.
17. Bulté L, Gans P, Rebeillé F, Wollman FA (1990) ATP control on state transitions *in vivo* in *Chlamydomonas reinhardtii*. *Biochim Biophys Acta* **1020:**72-80.
18. Cardol P, Gloire G, Havaux M, Remacle C, Matagne R, Franck F (2003) Photosynthesis and state transitions in mitochondrial mutants of Chlamydomonas reinhardtii affected in respiration. *Plant Physiol* **133:**2010-20.
19. Cardol P, Remacle C (2008) in *The Chlamydomonas Source Book 3*, eds. Stern D, Harris EE (Elsevier, Vol. 2, Organellar and Metabolic Processes.
20. Dietzel L, Brautigam K, Pfannschmidt T (2008) Photosynthetic acclimation: state transitions and adjustment of photosystem stoichiometry--functional relationships between short-term and long-term light quality acclimation in plants. *Febs J* **275:**1080-8.
21. Joliot P, Delosme R (1974) Flash-induced 519 nm absorption change in green algae. *Biochim Biophys Acta* **357:**267-84.
22. Butler WL (1978) Energy distribution in the photochemical apparatus of photosynthesis. *Ann rev Plant Physiol* **29:**345-78.
23. Samson G, Bruce D (1995) Complementary changes in absorption cross-sections of Photosystems I and II due to phosphorylation and Mg2+-depletion in spinach thylakoids. *Biochim Biophys Acta* **1232:**21-6.
24. Finazzi G, Sommer F, Hippler M (2005) Release of oxidized plastocyanin from photosystem I limits electron transfer between photosystem I and cytochrome b6f complex in vivo. *Proc Natl Acad Sci U S A* **102:**7031-6.
25. Joliot P, Joliot A (2006) Cyclic electron flow in C3 plants. *Biochim Biophys Acta* **1757:**362-8.
26. Jans F, Mignolet E, Houyoux PA, Cardol P, Ghysels B, Cuine S, Cournac L, Peltier G, Remacle C, Franck F (2008) A type II NAD(P)H dehydrogenase mediates light-independent plastoquinone reduction in the chloroplast of Chlamydomonas. *Proc Natl Acad Sci U S A*.
27. Genty B, Harbinson J, Briantais J-M, Baker NR (1990) The relationship between non-photochemical quenching of chlorophyll fluorescence and the rate of photosystem 2 photochemistry in leaves. *Photosynth Res* **25:**249-57.

28. Maxwell PC, Biggins J (1976) Role of cyclic electron transport in photosynthesis as measured by the photoinduced turnover of P700 in vivo. *Biochemistry* **15:**3975-81.
29. Lemaire C, Wollman FA, Bennoun P (1988) Restoration of phototrophic growth in a mutant of Chlamydomonas reinhardtii in which the chloroplast atpB gene of the ATP synthase has a deletion: an example of mitochondria-dependent photosynthesis. *Proc Natl Acad Sci U S A* **85:**1344-8.
30. Allen JF (2003) Cyclic, pseudocyclic and noncyclic photophosphorylation: new links in the chain. *Trends Plant Sci* **8:**15-9.
31. Steigmiller S, Turina P, Graber P (2008) The thermodynamic H+/ATP ratios of the H+-ATPsynthases from chloroplasts and Escherichia coli. *Proc Natl Acad Sci U S A* **105:**3745-50.
32. Arnon DI (1959) Conversion of light into chemical energy in photosynthesis. *Nature* **184:**10-21.
33. Ort DR, Baker NR (2002) A photoprotective role for O(2) as an alternative electron sink in photosynthesis? *Curr Opin Plant Biol* **5:**193-8.
34. Noguchi K, Yoshida K (2008) Interaction between photosynthesis and respiration in illuminated leaves. *Mitochondrion* **8:**87-99.
35. Forti G, Furia A, Bombelli P, Finazzi G (2003) In vivo changes of the oxidation-reduction state of NADP and of the ATP/ADP cellular ratio linked to the photosynthetic activity in Chlamydomonas reinhardtii. *Plant Physiol* **132:**1464-74.
36. Dutilleul C, Driscoll S, Cornic G, De Paepe R, Foyer CH, Noctor G (2003) Functional mitochondrial complex I is required by tobacco leaves for optimal photosynthetic performance in photorespiratory conditions and during transients. *Plant Physiol* **131:**264-75.
37. Witt HT (1979) Energy conversion in the functional membrane of photosynthesis. Analysis by light pulse and electric pulse methods. The central role of the electric field. *Biochim Biophys Acta* **505:**355-427.

FIGURE LEGENDS

Figure 1. Impact of inhibition of the mitochondrial respiratory-chain on growth of ST-deficient strain. Cells were cultivated at 50 µmol photons m^{-2} s^{-1} in mixotrophic (TAP) or photoautotrophic (Min) conditions in the absence or presence (+M) of the mitochondrial respiratory inhibitor myxothiazol (5µM). ***A.*** Drops of cell suspensions (A_{750nm} ~ 0.01) were plated on solid media and growth was estimated after 3-5 days. ***B.*** doubling time in liquid cultures. Error bars indicate standard deviation of the mean of 3 independent measurements. ***C***. Same experimental procedure as in panel A. Photoautrotrophic (Min) conditions. Light intensity was either 50 or 400 µmol photons m^{-2} s^{-1}.

Figure 2. Comparative analysis of the photosynthetic features of *dum22 stt7-9* *A*. PSII/PSI ratios. Changes in the amplitude of the fast phase of the ECS signal (at 520–545 nm) upon excitation with a saturating laser flash in the presence or absence of PSII inhibitors DCMU (20µM) and hydroxylamine (1mM) were used to assess PSI and PSII stoichiometry. ***B.*** **PSII relative antenna size**, as evaluated form fluorescence induction kinetics. Curves were normalized to the same value of variable fluorescence to allow a better comparison. Closed squares: wild type; open circles: *stt7-9*; downwards grey triangles: *dum22*; upwards crossed triangles: *dum22 stt7-9*. ***C.*** **effect of preillumination on PSII relative antenna size in *dum22* and *dum22 stt7-9* cells**. Solid symbols: dark adaptation for 20 minutes under strong agitation. Open symbols: exposure to 50µmol m^{-2} s^{-1} for 10 minutes in presence of DCMU 10µM. Downwards triangles: *dum22*. Upwards triangles: *dum22 stt7-9*. ***D.*** **PSI antenna size** as evaluated form the light saturation curve for P700 oxidation in intact cells. The curves were acquired by flashing the cells with laser light of varying intensity and measuring the resulting P700 oxidation. Traces were measured in the presence of hydroxylamine (1 mM) and DCMU (20µM) to prevent PSII charge separation. Same symbols as in panel B.

Figure 3 Electron transfer reactions in continuous light. *A.* P_{700} oxidation kinetics measured in continuous light in the presence of MV (2 mM). Open symbols: 50µmol m^{-2} s^{-1}; solid symbols: 800 µmol m^{-2} s^{-1}. Black box: actinic light off; white box: actinic light on. ***B***: **light saturation of P_{700} oxidation** evaluated from data as in panel A. The time at which the light was switched off was taken as time zero. Closed squares: wild type; open circles: *stt7-9*; downwards grey triangles:

dum22; upwards crossed triangles: *dum22 stt7-9*. ***C.*** **Light saturation curves of oxygen evolution in** wild type**, *stt7-9*, *dum22* and *dum22 stt7-9* cells**. Photosynthetic activity was calculated as ‘‘net photosynthesis’’ (*i.e.*, photosynthesis after correction for respiration) at any given light intensity. ***D.*** **ΦPSII**, calculated as (*Fm*-*Fs*)/*Fm*. Error bars indicate standard error of the mean of three independent measurements.

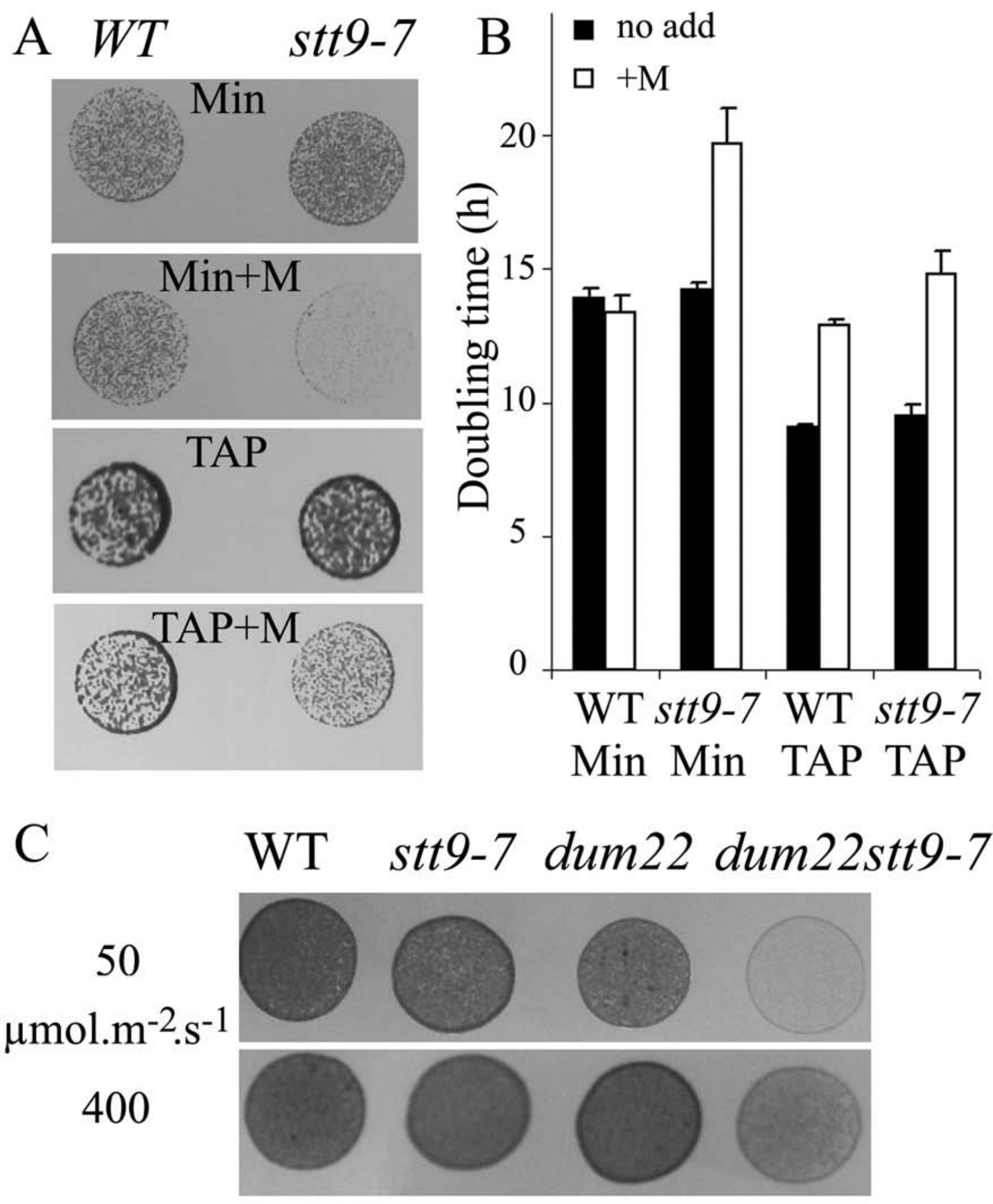
A
WT
stt9-7
Min
Min+M
TAP
TAP+M
B
no add
+M
Doubling time (h)
0
5
10
15
20
WT
stt9-7
WT
stt9-7
Min
Min
TAP
TAP
C
WT
stt9-7
dum22
dum22stt9-7
50
µmol.m-2.s-1
400

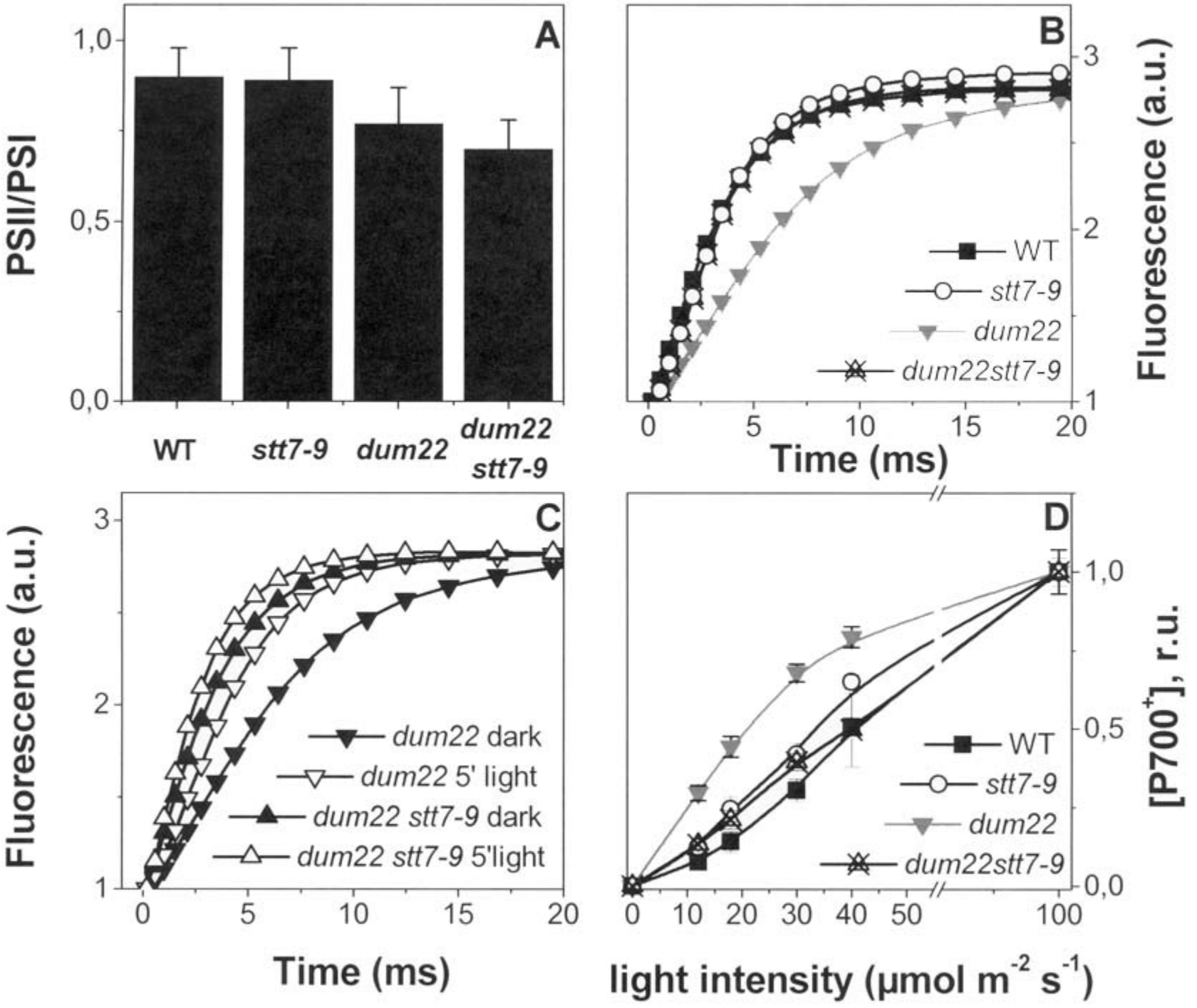
A
PSII/PSI
1,0
0,5
0,0
WT
stt7-9
dum22
dum22 stt7-9
B
Fluorescence (a.u.)
Time (ms)
WT
stt7-9
dum22
dum22stt7-9
C
Fluorescence (a.u.)
Time (ms)
dum22 dark
dum22 5' light
dum22 stt7-9 dark
dum22 stt7-9 5'light
D
[P700+], r.u.
light intensity (µmol m-2 s-1)
WT
stt7-9
dum22
dum22stt7-9

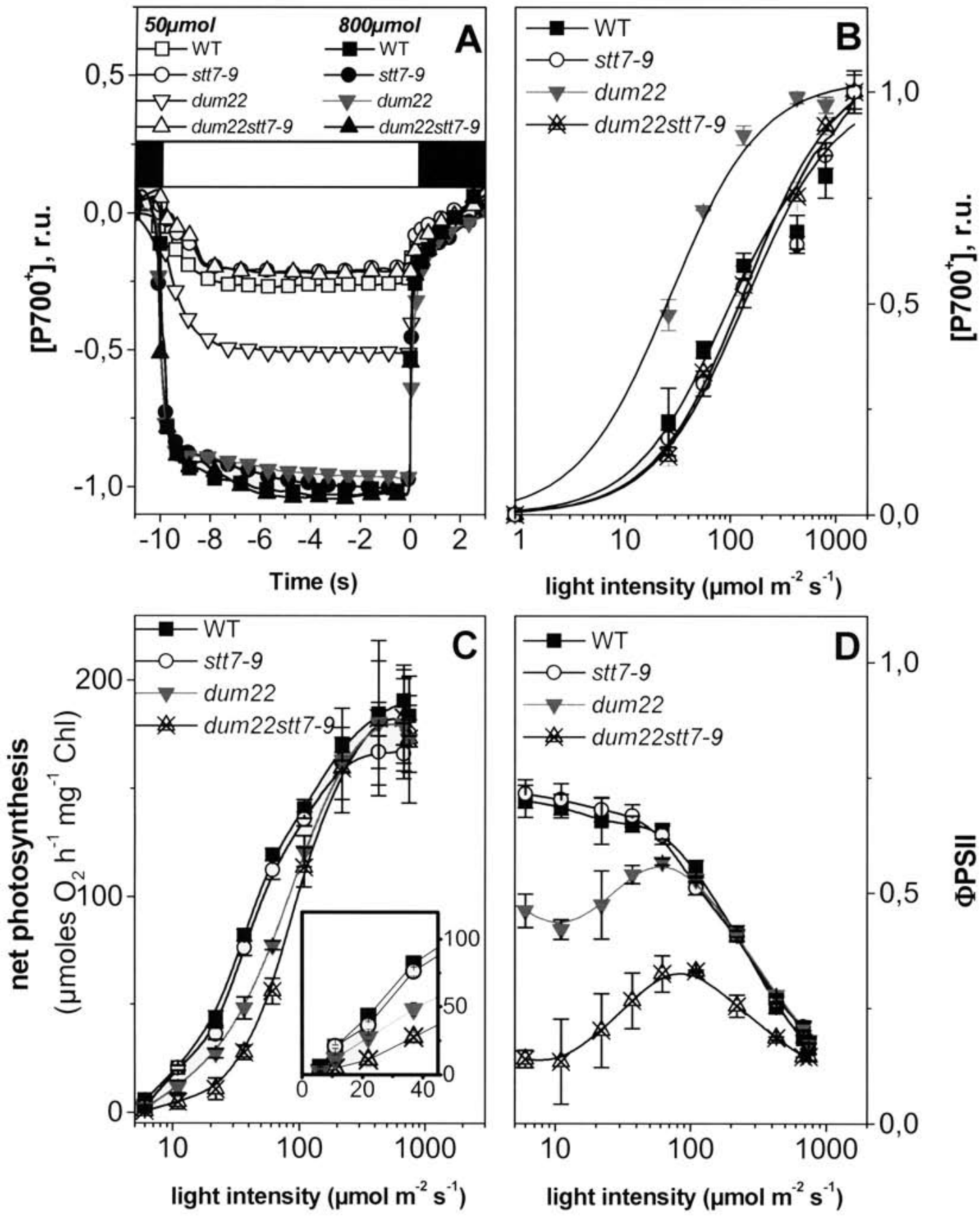
A
50µmol
800µmol
WT
stt7-9
dum22
dum22stt7-9
[P700+], r.u.
Time (s)
B
light intensity (µmol m-2 s-1)
C
net photosynthesis
(µmoles O2 h-1 mg-1 Chl)
D
ΦPSII

Table I. Relative cyclic electron flow (CEF) and cellular ATP content in wild type, *stt7-9*, *dum22* and *dum22 stt7-9* cells. CEF was evaluated as = k * $[P_{700}^{+}]/([P_{700}^{+}]+[P_{700}]$ after illumination in the presence of DCMU (20µM), where k represents the P_{700}^{+} re-reduction rate after steady state illumination of saturating intensity. CEF rates at low light (50µmol m^{-2} s^{-1}) are normalized to the maximum value (typically 12.5 ± 0.1 s^{-1} in wild type cells). Standard deviation is relative to at least 5 replicates. ATP is expressed in percentage of the wild-type control (107 ± 12 nmol mg Chl^{-1}). Cells were either fixed after 3h in the dark or after continuous illumination with low light (50 µmol m^{-2} s^{-1}).

Strain	CEF	ATP TAP dark	ATP TAP hν	ATP min hν
wild type	0.35 ± 0.05	66.2 ± 6.8	100	93.0 ± 9.1
stt7-9	0.37 ± 0.05	55.9 ± 6.1	102.3 ± 12.3	83.8 ± 20.4
dum22	0.63 ± 0.09	3.0 ± 1.3	69.0 ± 10.0	69.0 ± 10.0
dum22 stt7-9	0.35 ± 0.02	1.8 ± 2.1	65.7 ± 6.5	71.2 ± 2.7